Development 126, 3171-3181 (1999)
Printed in Great Britain © The Company of Biologists Limited 1999
DEV5304

UNC-84 localizes to the nuclear envelope and is required for nuclear migration and anchoring during *C. elegans* development

Christian J. Malone[1], William D. Fixsen[2,*], H. Robert Horvitz[2] and Min Han[1,‡]

[1]Howard Hughes Medical Institute, Department of Molecular, Cellular and Developmental Biology, University of Colorado at Boulder, Boulder CO 80309-0347, USA
[2]Howard Hughes Medical Institute, Dept. of Biology, Room 68-425, Massachusetts Institute of Technology, Cambridge MA 02139, USA
*Present address: Harvard University, 51 Brattle Street, Cambridge MA 02138, USA
‡Author for correspondence (e-mail: Mhan@colorado.edu)

Accepted 24 March; published on WWW 21 June 1999

SUMMARY

Nuclear migrations are essential for metazoan development. Two nuclear migrations that occur during *C. elegans* development require the function of the *unc-84* gene. *unc-84* mutants are also defective in the anchoring of nuclei within the hypodermal syncytium and in the migrations of the two distal tip cells of the gonad. Complementation analyses of 17 *unc-84* alleles defined two genetically separable functions. Both functions are required for nuclear and distal tip cell migrations, but only one is required for nuclear anchorage. The DNA lesions associated with these 17 mutations indicate that the two genetically defined functions correspond to two distinct regions of the UNC-84 protein. The UNC-84 protein has a predicted transmembrane domain and a C-terminal region with similarity to the *S. pombe* spindle pole body protein Sad1 and to two predicted mammalian proteins. Analysis of a green fluorescent protein reporter indicated that UNC-84 is widely expressed and localized to the nuclear envelope. We propose that UNC-84 functions to facilitate a nuclear-centrosomal interaction required for nuclear migration and anchorage.

Key words: Nuclear migration, *Caenorhabditis elegans*, *unc-84*, Nuclear anchoring

INTRODUCTION

Nuclear migration is essential for the movement of pronuclei during fertilization, for normal mitotic and meiotic cell division and for a variety of interphase functions (Morris et al., 1995). For example, interphase nuclear migration is essential for axis determination, embryogenesis and eye morphogenesis in *Drosophila melanogaster* and the morphogenesis of other epithelial structures, such as the vertebrate brain (reviewed by Morris et al., 1995).

Molecular and genetic analyses of nuclear migration in *Saccharomyces cerevisae*, *Aspergillus nidulans* and *Neurospora crassa* have revealed a conserved mechanism for fungal nuclear migration during interphase that depends upon the presence of intact microtubules (Morris et al., 1995; Oakley and Morris, 1980; Sullivan and Huffaker, 1992). The minus-end directed microtubule motor dynein and components of the dynein-associated dynactin complex are required for interphase nuclear migration (reviewed by Morris et al., 1995; Steinberg, 1998). Many proteins of unknown function are also important for fungal nuclear migration.

Much less is known about the mechanism of nuclear migration during metazoan development. In syncytial *Drosophila* embryos that lack nuclei because DNA synthesis and nuclear division have been blocked with aphidicolin, centrosomes undergo the movements of the normal nuclear-centrosomal complex, indicating that the force that produces nuclear movement could act through the centrosome (Raff and Glover, 1989). Pharmacological studies have implicated microtubules in a variety of metazoan nuclear migrations (Reinsch and Gonczy, 1998). Furthermore, dynein and dynactin appear to act in *Drosophila* nuclear migration: a dominant-negative allele of a dynactin component, *Glued[1]*, causes defects in nuclear migration in the *Drosophila* eye (Fan and Ready, 1997). Mutations in another *Drosophila* gene, *marbles/klarsicht*, also cause defects in nuclear migration (Fischer-Vize and Mosley, 1994; Welte et al., 1998); a molecular characterization of *marbles* has yet to be reported.

To address further the control of nuclear migration during animal development, we have undertaken the study of two sets of nuclear migrations that occur during *C. elegans* development. The first involves the embryonic formation of the dorsal hypodermal syncytium, hyp7. During the morphogenesis stage of embryogenesis, 17 of the 23 hyp7 cells initiate elongation by extending over the dorsal midline to a contralateral position (Fig. 1A). The cell continues to change shape until it forms an elongated strip over the dorsal surface of the embryo. The nucleus then migrates to the contralateral position within the cytoplasm (Sulston et al., 1983). The

progression of hyp7 cell elongation is microtubule-independent, while the subsequent nuclear migration is microtubule-dependent (Williams-Masson et al., 1998). After cell elongation and nuclear migration, the cells fuse to form a syncytium.

The second set of nuclear migrations we have studied occurs during the migration of the P cells (Fig. 1B). A newly hatched larva has a ventrolateral row of six P cell nuclei on each side. During the mid-L1 larval stage, these nuclei migrate to the ventral cord. After the nucleus migrates, the remaining cell body follows such that the 12 P cells form a single row along the ventral cord (Sulston and Horvitz, 1977; Sulston, 1976).

Many mutations have been identified that specifically affect these two nuclear migrations (Horvitz and Sulston, 1980; also see Materials and Methods). These mutations define two genes, *unc-83* and *unc-84*. The initial characterization of *unc-83* and *unc-84* mutants indicated that the hyp7 and P cell movements initiate normally but that the subsequent nuclear migrations are defective (Sulston and Horvitz, 1981).

MATERIALS AND METHODS

Strains and genetic methods

Bristol N2 (Brenner, 1974) was used as the wild-type strain and as the parent of all mutant strains. Methods for the handling, culture, and genetic manipulation of animals were as described previously (Brenner, 1974). Experiments were performed at 15° and 25°C, as indicated.

Most mutants were isolated after mutagenesis of N2 with ethyl methanesulfonate (EMS) (Brenner, 1974). The isolation of *unc-84(e1174, e1410, e1411, e1412, n296, n321, n322, n323, n369, n399, n400)* has previously been described (Horvitz and Sulston, 1980; Sulston and Horvitz, 1981; Trent et al., 1983). *unc-84(n1221)* arose spontaneously and *unc-84(n1219, n1220)* were isolated by C. Desai in the laboratory of H. R. H. *unc-84(e1748)* was isolated based upon its defect in hyp7 nuclear migration during a screen for mutants using Nomarski DIC microscopy by E. Hedgecock (personal communication). *unc-84(sa60, sa61)* were isolated in an unrelated screen by D. Reiner and J. Thomas (personal communication).

Phenotypic analysis

Defects in P cell migration were quantified by counting the neuronal descendants of the P cells. From the number of neurons in the ventral cord, we subtracted 15, the number of neurons present before P cell migration (Sulston and Horvitz, 1977). The resulting number was divided by 42, the number of neurons derived from the P cells in a wild-type animal (Sulston and Horvitz, 1977) to give a measure of the expressivity of the P cell nuclear migration defect. The defect in hyp7 nuclear migration was quantified by counting the number of hyp7 cell nuclei in the dorsal cord. This number was subtracted from 16, the number of hyp7 nuclei that would be present if all migrations failed (Sulston et al., 1983), and divided by 16 to indicate the percentage of nuclear migrations that were normal.

Complementation analyses were performed on all pairwise combinations of 12 alleles (Table 2). Five additional alleles (*n1325, n1410, n1538, sa60* and *sa61*) were tested using representative alleles from each of the four classes: 1, *n369;* 2, *n371;* 3, *n321;* and 4, *e1174*.

The seam cell nuclear anchoring defect was observed using the seam cell marker in the strain JR672. This green fluorescent protein (GFP) marker is expressed in all seam cells, from their time of specification through their time of fusion into a syncytium during the final larval molt (Terns et al., 1997). A seam cell syncytium was scored as mutant if any nucleus appeared to touch a neighboring nucleus. The gonadal migration defect was scored by observing the position of a mutant gonad using Nomarski optics and comparing it to the invariant C-shape of a wild-type gonad. If any significant differences were observed, it was scored as defective.

Cloning, northern blot analysis and cDNA isolation

Cosmids in the region defined by the physical mapping of *mnDp1*, *mnDp9* and *mnDp27* were injected at concentrations of 5-20 ng/ml with the dominant co-transformation marker pRF4 at 65 ng/ml into the germlines of *unc-84(e1410)* animals (Mello and Fire, 1995).

pCM9 was used as a probe for a northern blot (courtesy of M. Sundaram). pCM9 and pCM10 were used to screen 7.5×10^5 plaques from an early embryonic cDNA library (courtesy of P. Okkema and A. Fire). Of 30 positive plaques, five were characterized. Two corresponded to the 3.5 kb class of cDNA, and three corresponded to the 2.5 kb class of cDNA. One full-length transcript of each class was identified.

5′ RACE of human cDNAs

The two human cDNAs with predicted similarity to the C terminus of UNC-84A were identified with a BLAST search of the EST database (Altschul et al., 1997; Boguski et al., 1993). Nested primers were designed based on the EST sequence for 5′ RACE. cDNAs were amplified from a human brain cDNA library, and their sequences were determined (Orita et al., 1995).

DNA sequence analysis and identification of mutant lesions

The sequence of a cDNA of each class was determined and compared to the sequence of the cosmid F54B11 (Waterston and Sulston, 1995) to confirm the sequence of the cDNAs and to determine exon/intron boundaries. The sequences of UNC-84A, Sad1, SUN1 and SUN2 were aligned using clustalw multiple sequence alignment (Thompson et al., 1994). To identify the molecular lesions of *unc-84* alleles, all exons and exon/intron boundaries were amplified using the polymerase chain reaction from genomic preparations of mutant DNA and purified by low melting point agarose electrophoresis. Their sequences were directly determined.

cDNA expression

We created two constructs to express either the UNC-84A or UNC-84B transcript under the control of the *hsp*16-2 promoter (pPD49.78, generously provided by A. Fire, Carnegie Institution of Washington). We introduced these constructs individually and together into an *unc-84(n369)* mutant strain using germline transformation (Mello and Fire, 1995) with the dominant transformation marker *sur-5::GFP* (pTG96) (Gu et al., 1998). Established transgenic lines that were raised at 25°C were subjected to heat-shock at 37°C for 80 minutes during the early L1 stage, before the P cell nuclear migration occurs.

GFP fusion construct

We constructed a clone that contained 11.5 kb of *unc-84* genomic DNA. The stop codon of the UNC-84A encoding transcript was replaced with a restriction site that was fused with the GFP coding sequence and an *unc-54* 3′ UTR (in the vector pPD95.72) (A. Fire, S. Xu, J. Ahnn and G. Seydoux, personal communication). We injected this construct into *dpy-20(e1282)* animals at 10 ng/ml along with the transformation marker pMH86, a subclone of the wild-type *dpy-20* gene (Han and Sternberg, 1990). The analysis of several extrachromosomal arrays indicated that this construct could fully rescue both *unc-84(n369)* and *unc-84(n321)* mutants and had identical expression patterns in all lines. An extrachromosomal array was integrated and shown to rescue. This integrated array (*kuIs32*) was used for all analyses presented here.

RESULTS

unc-84 affects two sets of nuclear migrations

Hyp7 nuclei often fail to migrate normally in *unc-84* mutant animals (Fig. 1A and Table 1) (Sulston and Horvitz, 1981). Although cytoplasmic processes seem to extend normally, the nuclei move slowly and reach only the dorsal midline (Fig. 2C,D). In contrast, the corresponding nuclei in wild type move substantially past the dorsal midline. The limited migration that does occur might be a passive consequence of pressure from adjacent muscle cells (Sulston and Horvitz, 1981). The abnormal positions of these nuclei do not cause any other apparent defects. Because these cells later fuse to form the hyp7 syncytium whether or not their nuclei have migrated normally, the role of nuclear migration in normal hyp7 development is not clear.

The 12 P cell nuclei also often fail to migrate in *unc-84* mutant animals (Fig. 1B and Table 1). Because P cells that fail in nuclear migration often die, *unc-84* animals are both uncoordinated (Unc) and egg-laying defective (Egl) as a consequence of the missing neurons and vulval precursor cells that otherwise would be generated by the P cells (Horvitz and Sulston, 1980; Sulston and Horvitz, 1981).

We examined P cell nuclear migration in *unc-84(e1410)* and *unc-84(e1411)* animals using Nomarski optics. Mutant P cell nuclei initiated nuclear movement but, during failed migrations, the nucleus always arrested midway through the cellular extension and, in most cases, returned to its original sub-lateral position, where the nucleus and remaining cell body subsequently died. These deaths appeared morphologically distinct from normal programmed cell deaths and were not affected by the *ced-3(n717)* mutation (data not shown), which prevents programmed cell death (Ellis and Horvitz, 1986). Furthermore, as reported previously (Sulston and Horvitz, 1981), cellular fragments appeared in the ventral cord at the positions normally occupied by the P cell nuclei. The deaths of the lateral P cell bodies, which did not undergo nuclear migration, may result from the loss of cellular components to these fragments in the ventral cord. Consistent with this hypothesis is the observation that *unc-40* mutant P cells, which are defective in all aspects of P cell migration, typically do not die (Hedgecock et al., 1990). In *unc-40; unc-84* mutant animals sub-lateral P cells live and divide (our unpublished observation). This result suggests that it is the failure of nuclear migration rather than the absence of *unc-84* activity that causes misplaced P cells to die in an *unc-84* mutant.

We characterized the migrations of both P cell and hyp7 nuclei for 17 *unc-84* alleles. Because each P cell normally gives rise to four or five ventral cord neurons, the number of neurons in the ventral cord can be counted as a measure of successful P cell nuclear migrations. The incorrect positioning of hyp7 nuclei in the dorsal cord of L1 larvae can be used to assess the frequency of the failure of hyp7 nuclear migrations (Fig. 2C,D). All *unc-84* alleles cause temperature-sensitive defects in the migrations of the P cell nuclei and defects in the hyp7 migrations at all temperatures (Table 1).

The temperature-sensitive period (TSP) for *unc-84(sa60)* for the defect in P cell migration is approximately the mid-L1 larval stage (Fig. 2G), the time at which P cells migrate into the ventral cord. Since all 17 alleles of *unc-84*, many of which appear to be molecular nulls (see below), are temperature sensitive for the P cell nuclear migration defect, we conclude that in the absence of *unc-84* function the process of P cell nuclear migration is inherently temperature sensitive.

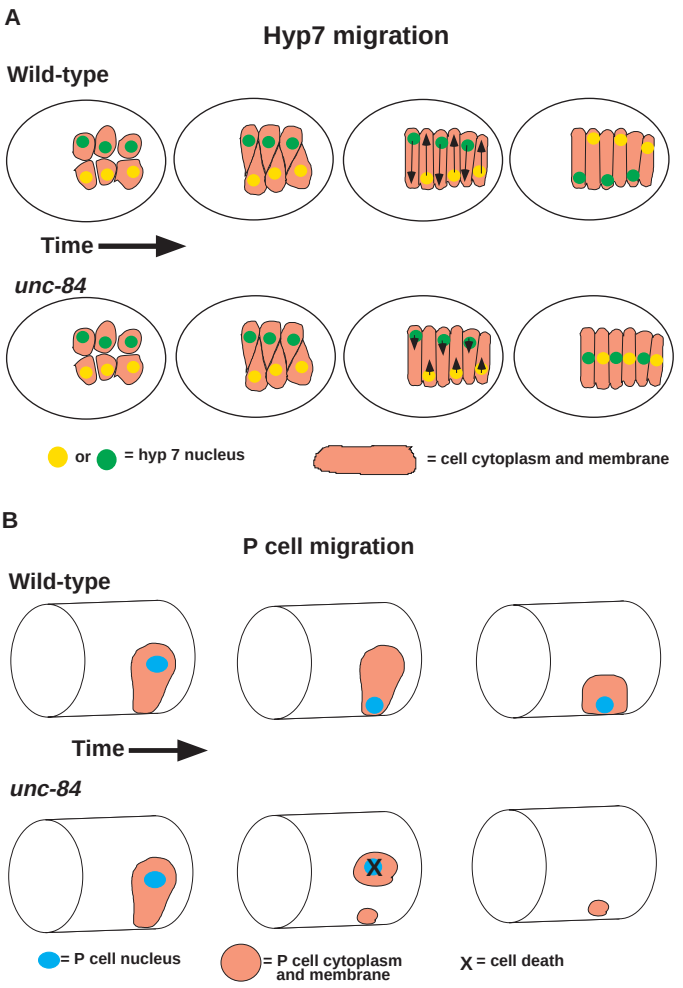

Fig. 1. Diagrams illustrating the two sets of nuclear migrations affected by *unc-84* mutations. Anterior is to the left. (A) Dorsal views of six representative (of 17 total) hyp7 precursor cells undergoing cell elongation and nuclear migration. Top, in a wild-type embryo. Bottom, in an *unc-84* embryo. Four stages are shown for each. (B) Left lateral views of three stages of one (of 12 total) P cell and nuclear migration. Top, in a wild-type L1 larva. Bottom, in an *unc-84* larva.

unc-84 controls two genetically separable functions

The defect in nuclear migration is corrected to varying degrees in particular *unc-84 trans*-heterozygotes. The presence or absence of such intragenic (or interallelic) complementation allowed us to assign the 17 alleles to one of four classes (Table 2). Suggesting that they abolish all *unc-84* functions, class 1 alleles failed to complement not only themselves but also all alleles of the other classes. In contrast, class 4 alleles complemented class 3 alleles completely and class 2 alleles weakly, indicating that class 3 alleles and class 4 alleles affect distinct functions of *unc-84* and that the class 2 and 3 alleles affect the same function. Molecular analysis of the class 1, 3

Table 1. Expressivity of defects in nuclear migration and anchoring of *unc-84* and *unc-83* mutants

Genotype[a]	Class[b]	% cell nuclei having migrated normally			% of animals with evenly distributed nuclei in the dorsal cord[e]
		hyp7[c]	P cell (25°C)[d]	P cell (15°C)	
n369	1	6	24	90	8
n400	1	6	14	88	38
n1325	1	3	43	85	0
n1410	1	5	31	70	23
n1538	1	10	45	88	36
sa60	1	15	20	75	25
e1412	2	13	52	80	40
n296	2	6	27	80	0
n323	2	9	27	83	0
n371	2	7	24	95	22
e1410	3	8	10	80	8
n321	3	6	27	86	39
n399	3	8	22	86	30
sa61	3	7	52	93	14
e1411	4	52	43	76	100
e1174	4	44	46	88	83
n322	4	46	41	93	100
unc-83(e1408)		5	21	86	100
wild-type		100	100	100	n.a.

For all data points presented, at least ten animals were scored and standard deviations were less than or equal to ±10%.
[a]Genotype is *unc-84* unless otherwise specified.
[b]*unc-84* alleles class (see Table 2).
[c]The percentage of normal hyp7 nuclear migrations (see Materials and Methods) was determined for animals raised at both 15° and 25°C. The results were statistically identical so the data were combined.
[d]See Materials and Methods.
[e]An animal was scored as aberrant if two adjoining nuclei were observed (as in Fig. 2C,D). An animal was scored as having evenly distributed nuclei if no adjoining nuclei were observed (as in Fig. 2B). In N2, the hyp7 nuclei migrate normally and therefore they are not present in the dorsal cord.
n.a., not applicable.

Table 2. Expressivity of hyp7 and P cell nuclear migration defects of inter se combinations of 12 *unc-84* alleles

		n400	*n369*	*n371*	*n323*	*n296*	*e1412*	*n399*	*n321*	*e1410*	*n322*	*e1411*	*e1174*
1	*n400*	6 14											
	n369	6 13	6 18										
	n371	11 12	4 21	7 24									
2	*n323*	9 17	8 45	11 30	9 20								
	n296	4 10	7 16	8 25	6 29	6 27							
	e1412	7 28	6 46	4 48	11 32	6 50	13 52						
	n399	8 13	5 18	23 20	24 26	17 22	24 48	8 22					
3	*n321*	8 17	6 29	11 20	13 46	14 40	21 50	6 24	6 29				
	e1410	1 9	6 16	4 9	7 25	13 19	13 36	9 20	7 28	8 10			
	n322	18 22	21 32	26 51	38 62	23 60	57 63	98 95	97 95	96 86	46 41		
4	*e1411*	20 19	16 26	30 62	36 65	15 55	53 81	97 100	98 99	94 96	51 42	52 51	
	e1174	73 25	24 23	38 60	34 58	21 58	53 74	99 95	98 99	95 87	47 51	52 50	44 46
		1			**2**				**3**			**4**	

	1	**2**	**3**	**4**
1	–			
2	–	–		
3	–	–	–	
4	–	+/–	+	–

For each allelic combination, the top number indicates the percent of successful hyp7 nuclear migrations and the bottom number indicates the percent of successful P cell migrations as scored by the P cell neuronal daughters. The alleles have been grouped according to their behaviors and designated with an arbitrary allele class number. We tested five additonal alleles with a representative from each class (see Materials and Methods). *n1325*, *n1410*, *n1538* and *sa60* are class 1 alleles and *sa61* is a class 3 allele. The small table on the upper right is a summary of the complementation data for the four classes. For all data points presented, at least 10 animals were scored and standard deviations were less than or equal to ±9%.

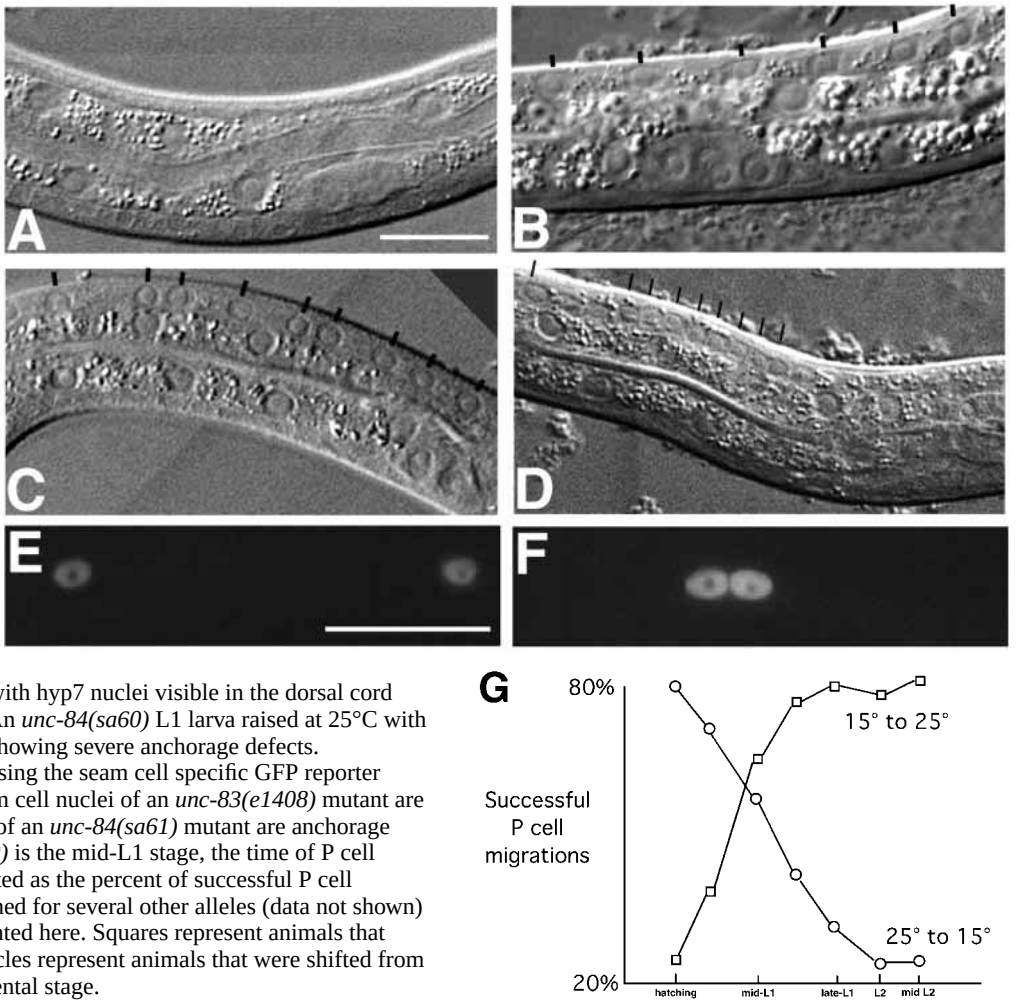

Fig. 2. *unc-84* mutant animals display defects in nuclear anchoring, and the TSP of *unc-84* for the P cell migration defect corresponds to the time of P cell migration. (A-D) Nomarski images of the dorsal cords of L1 larvae. Equivalent focal planes are presented as evidenced by the gonad primordium and ventral cord neurons. hyp7 nuclei are indicated by black bars. Bar, 10 μm. (A) A wild-type L1 larva with no hyp7 nuclei present in the dorsal cord. The nuclei are in their normal dorsal-lateral positions on either side of this focal plane. (B) An *unc-83(e1408)* L1 larva with hyp7 nuclei visible in the dorsal cord and anchored at regular intervals along the anterior-posterior axis. (C) An *unc-84(sa60)* L1 larva raised at 15°C with hyp7 nuclei visible in the dorsal cord showing mild anchorage defects. (D) An *unc-84(sa60)* L1 larva raised at 25°C with hyp7 nuclei visible in the dorsal cord showing severe anchorage defects. (E,F) Seam cell nuclei of adults expressing the seam cell specific GFP reporter from strain JR672. Bar, 5 μm. (E) Seam cell nuclei of an *unc-83(e1408)* mutant are regularly spaced. (F) Seam cell nuclei of an *unc-84(sa61)* mutant are anchorage defective. (G) The TSP of *unc-84(sa60)* is the mid-L1 stage, the time of P cell nuclear migration. The data are presented as the percent of successful P cell migrations. The TSP was also determined for several other alleles (data not shown) and was consistent with the data presented here. Squares represent animals that were shifted from 15° to 25°C, and circles represent animals that were shifted from 25° to 15°C at the indicated developmental stage.

and 4 alleles is consistent with this genetic inference (see below).

unc-84 is involved in nuclear anchoring and gonad migration

In addition to the nuclear migration defects of *unc-84* animals, we observed that nuclei of the hyp7 syncytium were often mispositioned and appeared to be unanchored within the cell, allowing them to move throughout the cytoplasm. This phenotype is very similar to that of *anc-1* (*anc*, anchorage defective) animals (Hedgecock and Thomson, 1982). We have quantified this phenotype for the 17 alleles of *unc-84* by scoring the percentage of animals in which hyp7 nuclei that are present in the dorsal cord appear to touch (Fig. 2D). In a wild-type hyp7 syncytium, nuclei never appear to touch (Hedgecock and Thomson, 1982). We observed that all class 1, 2 and 3 alleles but no class 4 alleles have severe anchoring defects (Table 1). Interestingly, *unc-83* mutants share the nuclear migration defects with *unc-84* mutants, but not the nuclear anchoring defects (Table 1). In contrast, *anc-1* mutations do not cause nuclear migration defects but do cause nuclear anchoring defects within hyp7 (Hedgecock and Thomson, 1982).

Because *anc-1* animals do not have hyp7 nuclei in the dorsal cord, to compare the nuclear anchoring defects of *unc-84* and *anc-1* animals, we scored the nuclei of the adult seam cells, which had previously been observed to be affected by *anc-1* (Hedgecock and Thomson, 1982) and which we found also to be affected in *unc-84* animals. We identified seam cell nuclei using a green fluorescent protein (GFP) marker that is expressed in seam cells (Terns et al., 1997). In this way, we could compare the effects of mutations in *anc-1*, *unc-83* and *unc-84* on nuclear anchoring independently of their effects on nuclear migration. Class 1, 2 and 3 *unc-84* alleles and the *anc-1(e1753)* mutation affected seam cell nuclear anchoring similarly (Table 3). The class 4 *unc-84* alleles and *unc-83* alleles did not affect seam cell nuclear anchoring (Table 3). We conclude that class 3 but not class 4 alleles affect an *unc-84* function required for nuclear anchoring and that *unc-83* is not required for nuclear anchoring. As predicted from these data, an *unc-83 anc-1* double mutant is indistinguishable from an *unc-84* mutant (data not shown).

We also observed a temperature sensitive gonadal migration defect for all allele classes of *unc-84*. The C-shape of the wild-type hermaphrodite gonad results from the migrations of the distal tip cell (DTC) at each end of the developing gonad (Hirsh et al., 1976; Kimble and Hirsh, 1979). In *unc-84* animals raised at 25°C, most gonad arms displayed an aberrant DTC migratory path (Table 3). While gonadal outgrowth proceeded with apparently normal kinetics, we observed that the gonadal arms displayed morphological abnormalities indicative of

Table 3. Characterization of nuclear anchoring and temperature-sensitive gonadal migration defects of *unc-84, unc-83* and *anc-1* animals

Genotype	Allele class	%WT seam cell position	%WT gonad migration 15°	%WT gonad migration 25°
unc-84(n369)	1	26	85	47
unc-84(sa60)	1	8		
unc-84(n296)	2	25		
unc-84(n371)	2	13	89	43
unc-84(e1410)	3	17		
unc-84(n321)	3	27	90	37
unc-84(n399)	3	25		
unc-84(e1174)	4	100	94	33
unc-84(e1411)	4	89		
anc-1(e1753)		4	100	96
unc-83(e1408)		100	90	39
Wild-type		100	100	100

The percent of seam cell syncytia that had proper nuclear anchoring was determined by observing nuclei that were marked with the GFP seam cell marker from the strain JR672. Animals raised at either 15° or 25° were scored for normal gonad migration. Gonad migration was scored by observation of adult gonadal position and compared to the invariant gonadal position observed in wild-type (WT) animals. At least 15 seam cell syncytia or gonadal arms were observed for each data point and standard deviations were less than or equal to ±10%.

abnormal DTC migration throughout larval development. *unc-83* animals also displayed a gonadal migration defect that was largely temperature sensitive, while *anc-1* animals had normal DTC migration (Table 3).

unc-84 encodes a novel transmembrane protein with a conserved C terminus

unc-84 maps between *unc-9* and *unc-3* on the X chromosome (Horvitz and Sulston, 1980). We localized *unc-84* to a small physical region, based on our physical mapping of the complementing duplication *mnDp9* and the non-complementing duplication *mnDp26* (Fig. 3). We tested cosmids in this region for their abilities to rescue the Unc and Egl defects of *unc-84(e1410)* animals. One rescuing cosmid, W01D6, was identified. Subcloning defined a region of 12 kb that could completely rescue the Unc and Egl phenotypes of *unc-84* (*e1174, e1410, n369*) animals (Fig. 3).

Probing with pCM9, a 9 kb clone from this 12 kb region, we detected two transcripts of 3.5 and 2.5 kb on a northern blot (Fig. 3). These two transcripts were approximately equally abundant and were detected in embryonic and early larval stages and at lower levels in later larval stages and adults (Fig. 3 and data not shown). This same probe was used to screen a *C. elegans* embryonic cDNA library (Okkema and Fire, 1994).

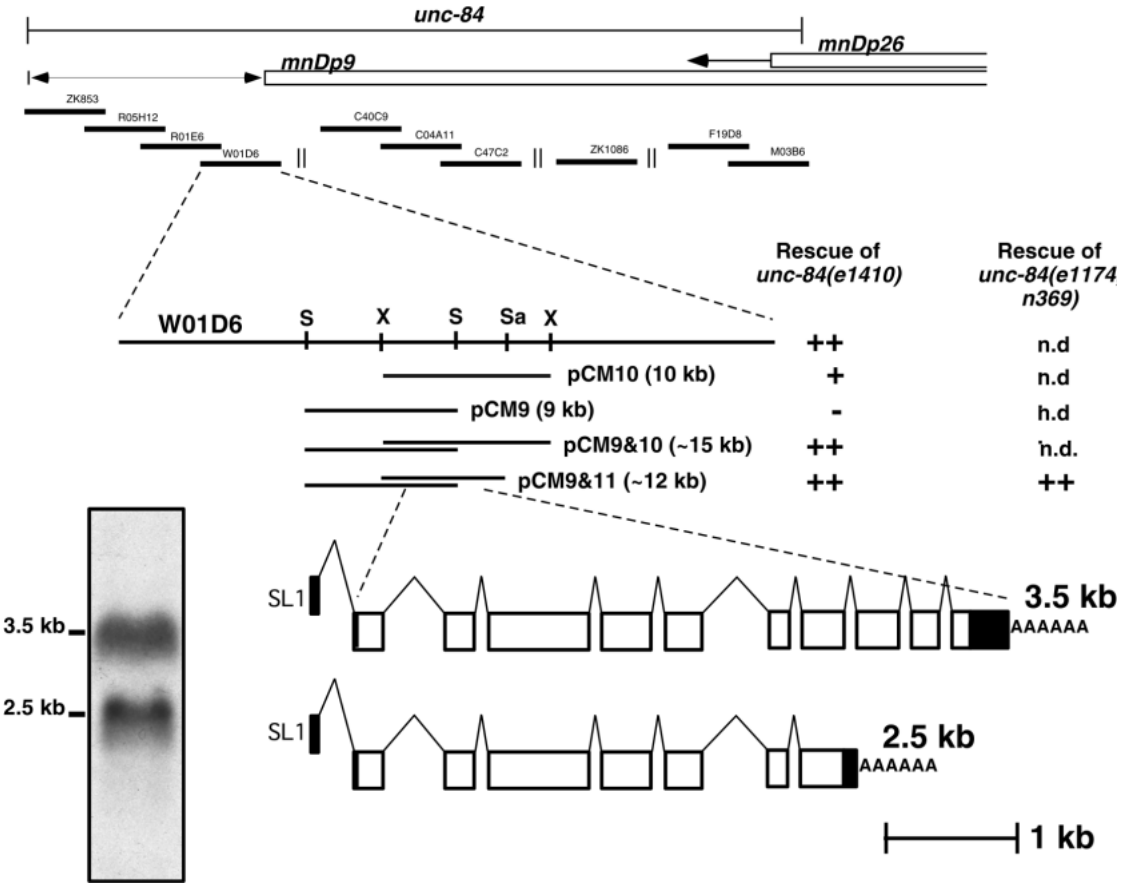

Fig. 3. Molecular characterization of *unc-84*. The duplication, *mnDp9*, complemented *unc-84*, while *mnDp26* failed to complement *unc-84*. We mapped the left end-point of *mnDp9* between cosmid ZK853 and W01D6, and we showed by Southern hybridization that *mnDp26* contains sequences within cosmid M03B6. Cosmids in this region were tested in transformation rescue experiments. One rescuing cosmid, W01D6, was identified. Subclones of W01D6 were assayed for rescue of *unc-84(e1174, e1410, n369)*. The genomic organization of the *unc-84* coding region is diagrammed below the rescuing subclones. The northern blot shows early embryonic poly(A) RNA probed with pCM9. Identical transcript sizes were observed when the northern blot was probed with pCM10 (data not shown), an overlapping clone required for rescued (Fig. 3). Based on the positions of ribosomal RNAs, the two transcripts are approximately 3.5 and 2.5 kb in length. Analysis of *unc-84* cDNAs shows that *unc-84* transcripts are *trans*-spliced to the *trans*-splice leader SL1 (Krause and Hirsh, 1987). Open boxes represent predicted open reading frames. Closed boxes represent the predicted untranslated regions. Relevant restriction sites in the *unc-84* region of W01D6 are diagrammed (X, *Xba*I; S, *Sal*I; Sa, *Sac*II).

Apparent full-length clones of both classes of transcripts were identified, based upon their sizes and on the presence of both a poly(A) tail and an SL1 splice-leader sequence (Krause and Hirsh, 1987). The two mRNAs are identical for the first 2.5 kb, with the longer transcript containing an additional 1 kb at its 3′ end (Fig. 3). The shorter transcript retains intron 7 of the longer transcript and is polyadenylated at a signal site within the retained intron. It is possible that the two transcripts are produced by alternative polyadenylation.

The long and short transcripts are predicted to encode polypeptides of 1,111 amino acids (aa) (UNC-84A) and 879 aa (UNC-84B) (Fig. 4). UNC-84A and B are identical for their first 876 aa. UNC-84A contains an additional 235 aa at its C terminus, and UNC-84B contains three unique aa (VTN) at its C terminus (Fig. 4). Both contain a potential membrane spanning hydrophobic region (aa 508-537).

Although searches of databases have not revealed a protein with an overall resemblance to UNC-84A, this protein has two striking features in common with Sad1, an essential protein required for normal spindle architecture from the yeast *Schizosaccharomyces pombe* (Hagan and Yanagida, 1995). The C-terminal 113 amino acids of UNC-84A share 34% identity and 74% similarity with the C terminus of Sad1 (Fig. 5A,B). Sad1 also has a predicted transmembrane domain and is associated with the *S. pombe* spindle pole body (analogous to the centrosome of animal cells) during all phases of the mitotic and meiotic cell cycle. Overexpressed Sad1 is localized to the nuclear periphery, suggesting that Sad1 is an integral nuclear envelope protein (Hagan and Yanagida, 1995). Sad1 has been hypothesized to anchor the spindle pole body to the nuclear envelope. No function has been assigned to the Sad1 C-terminal region, which shows similarity to UNC-84A.

We identified several mammalian genes with high similarity to the C terminus of UNC-84A by a BLAST search of the expressed sequence tag (EST) database (Altschul et al., 1997; Boguski et al., 1993). We cloned cDNAs for the two most similar genes from a human brain cDNA library (Orita et al., 1995). The predicted proteins, SUN1 and SUN2 (for Sad, UNC-84 domain protein), from each of these genes share 47% and 41% identity with the C-terminal 178 aa of UNC-84A (Fig. A,B). SUN1, SUN2, Sad1 and UNC-84 have no further regions of similarity. Interestingly, both SUN1 and SUN2 also have a predicted transmembrane domain (Fig. 5A). Although the UNC-84 C terminus may be conserved in mammals, worms and fission yeast, a search of the *S. cerevisae* database revealed no regions of similarity with the UNC-84A protein.

Molecular lesions define functional domains of UNC-84

To characterize physically the genetically separable functions defined by our complementation analysis of *unc-84* alleles and to confirm that we had cloned *unc-84*, we determined the sequences of the genomic DNA from the 17 *unc-84* mutant strains. A single mutation was identified for each allele of *unc-84*.

The six class 1 alleles, which failed to complement all others, cause in-frame stop codons that are distributed throughout the coding region of *unc-84* (Fig. 4). The four class 3 and three class 4 alleles, which completely complement each other, cluster in the C and N termini, respectively (Fig. 4). It

Fig. 4. UNC-84 sequence and mutations. The predicted UNC-84 protein products are shown. The putative membrane-spanning hydrophobic domain (508-537) is boxed. The C-terminal region with similarity to Sad1 and a family of human genes is underlined. The three amino acids unique to UNC-84B (VTN) are shown below the sequence of UNC-84A. All nonsense and missense alleles are identified with an asterisk above the amino acid they are predicted to affect. The in-frame deletion allele *e1174* is indicated by a thin line above the deleted amino acids. The deletion allele *n322*, which removes the predicted start ATG, is indicated by a thick line over the deleted amino acids. The next ATG is at aa 209 in a good ribosome binding site context and might initiate protein synthesis (Kozak, 1984). The 4 bp insertion allele *n1325* is indicated at the point of insertion. This allele is predicted to shift the frame +1, which would result in a truncated protein containing 13 abnormal amino acids. The allele *e1412* changes the splice acceptor of intron 2 from the consensus of tttcag to tttcaa. Each allele is color coded with regards to its complementation class. Class 1, red; Class 2, gray; Class 3, green; Class 4, blue.

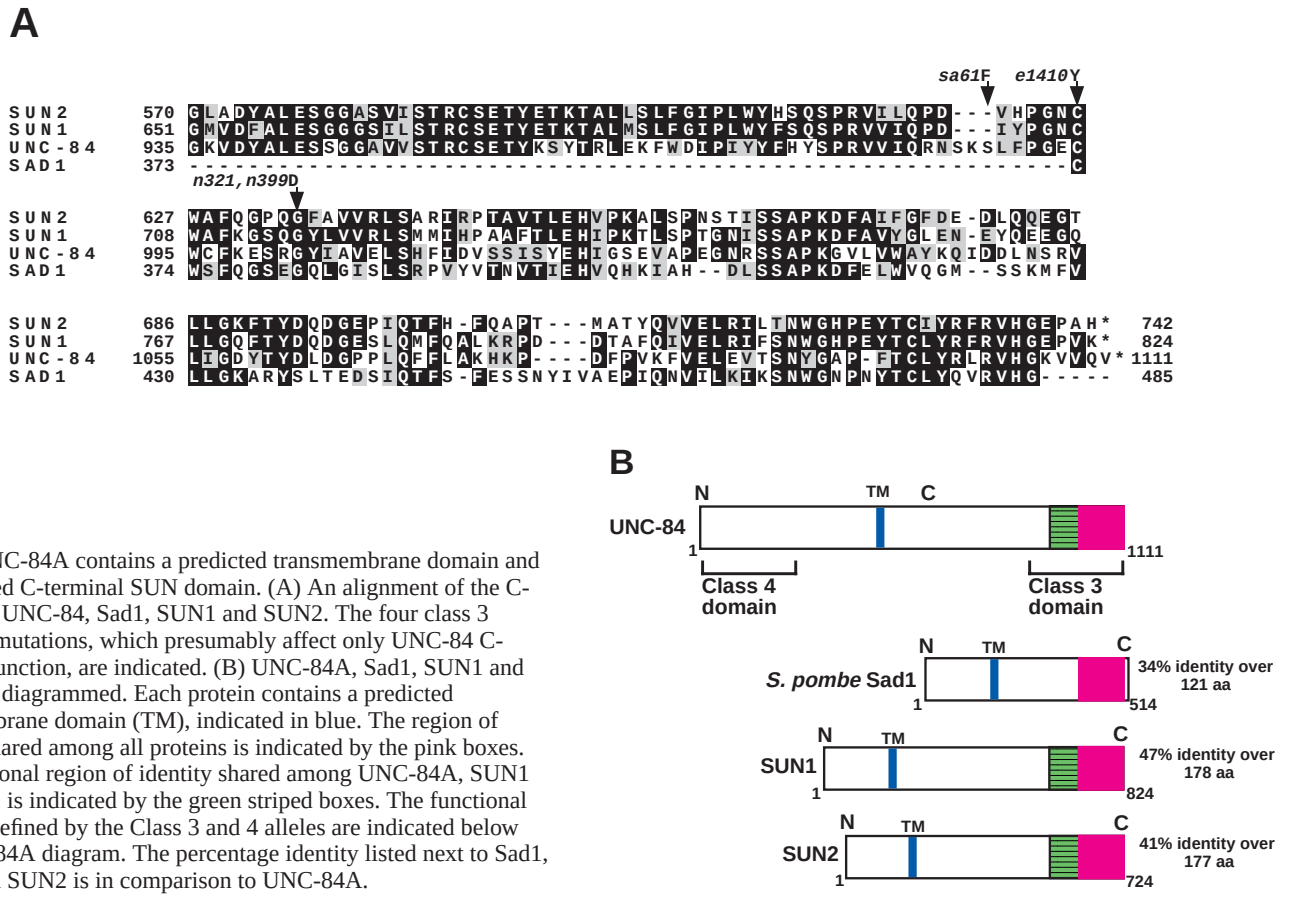

Fig. 5. UNC-84A contains a predicted transmembrane domain and a conserved C-terminal SUN domain. (A) An alignment of the C-termini of UNC-84, Sad1, SUN1 and SUN2. The four class 3 missense mutations, which presumably affect only UNC-84 C-terminal function, are indicated. (B) UNC-84A, Sad1, SUN1 and SUN2 are diagrammed. Each protein contains a predicted transmembrane domain (TM), indicated in blue. The region of identity shared among all proteins is indicated by the pink boxes. The additional region of identity shared among UNC-84A, SUN1 and SUN2 is indicated by the green striped boxes. The functional domains defined by the Class 3 and 4 alleles are indicated below the UNC-84A diagram. The percentage identity listed next to Sad1, SUN1 and SUN2 is in comparison to UNC-84A.

is likely that these mutations do not grossly affect protein levels or protein structure, since in *trans* together they can provide complete *unc-84* function. Of the class 4 alleles, two are deletions and one is a missense mutation. All three might affect only the N terminus (Fig. 4). Class 3 alleles are missense mutations that affect amino acids in the C-terminal region conserved in Sad1, SUN1 and SUN2. The four class 2 alleles include nonsense, missense and splice acceptor mutations that do not cluster (Fig. 4). It is possible that these mutations cause a partial loss of *unc-84* function and that such partial activity can weakly complement the defect in a class 4 mutation.

UNC-84A is necessary and sufficient for *unc-84* activity

The class 1 alleles *n400* and *n1538* are predicted to produce truncated proteins of 966 and 1,041 amino acids. If so, and if these proteins are stable, the C-terminal 70 amino acids of UNC-84A must be necessary for *unc-84* function. *n400* and *n1538* are not predicted to affect the short *unc-84* transcript, suggesting that the long transcript is necessary for all *unc-84* functions.

To determine if the UNC-84A transcript is sufficient for *unc-84* activity, the UNC-84A and UNC-84B cDNAs were independently expressed under the control of a heat shock promoter, *hsp*16-2, (Materials and Methods) in a strain homozygous for the class 1 allele *n369*. As a control, transgenic strains that expressed both transcripts were rescued for the unc-84 phenotype, as evidenced by the P cell migration success rate of 67% ±10% after heat shock compared to the non-transgenic control of 24% ±9%. Strains that expressed only the UNC-84B transcript were not rescued (P cell migration success rate of 24% ±16% after heat shock), suggesting UNC-84B is not sufficient for the *unc-84* function. In contrast, strains that expressed the UNC-84A transcript alone were rescued (P cell migration success rate of 56% ±12% after heat shock). The rescue experiments and analysis of the class 1 alleles suggest that the UNC-84A transcript is necessary and sufficient for *unc-84* function.

UNC-84A::GFP is widely expressed and concentrated at the nuclear periphery

To investigate the expression pattern and sub-cellular localization of UNC-84A, we expressed UNC-84A with a C-terminal GFP tag under the control of the endogenous promoter. This construct was able to rescue the Unc and Egl defects of *unc-84(e1410)* animals, indicating that the fusion protein was functional. UNC-84A::GFP was present in all somatic cell types examined in all larval stages and adults in both wild-type and *unc-84* mutant animals (Fig. 6). Consistent with the *unc-84* phenotype, UNC-84A::GFP was observed in P-cells during nuclear migration, the DTCs during migration (Fig. 6E,F) and the hypodermis during all stages of post-embryonic development (Fig. 6C,D).

In all cells observed, UNC-84A::GFP fluorescence was closely associated with and mostly uniformly distributed along the nuclear periphery (Fig. 6). This observation suggests that UNC-84 is a component of or is closely associated with the nuclear envelope. This localization was also observed in *unc-*

83 mutant strains, suggesting that *unc-83*, which causes a very similar phenotype to *unc-84*, is not required for UNC-84A localization.

DISCUSSION

We show here that *unc-84*, which functions in nuclear migration and anchoring in *C. elegans*, encodes a novel protein with a C-terminal region with similarity to the *S. pombe* spindle pole body protein Sad1 and to the products of a previously undescribed mammalian gene family. *unc-84* controls two genetically separable functions, which correspond to the N and C termini of the UNC-84A protein. Temperature-shift experiments suggest that UNC-84 acts at the time of migration. A functional UNC-84::GFP fusion protein localized to the nuclear periphery, suggesting that UNC-84 acts at the nuclear envelope during nuclear migration.

unc-84 putative null mutations are temperature sensitive for the P cell nuclear migration and the DTC migration but not for the hyp7 nuclear migration

We believe that *unc-84* class 1 alleles are null alleles, based on the expressivity of mutant phenotypes and our complementation and molecular analyses. These alleles cause a non-temperature sensitive defect in hyp7 nuclear migration and a temperature sensitive defect in P cell nuclear migration and in DTC migration. These data suggest that in the absence of *unc-84* function the process of P cell nuclear migration is temperature sensitive. Another gene product might be capable of providing *unc-84*-like function to allow P cell nuclear migration to occur at lower temperatures in the absence of *unc-84* activity but not be sufficient at higher temperatures.

UNC-84 may have two functional domains

Our complementation data define two genetically separable *unc-84* functions. Based on the molecular lesions associated with the alleles of *unc-84* that complement each other, we propose that the N and C termini of the UNC-84A protein are distinct functional domains. Although, the sequence of *unc-84* does not reveal a biochemical function for either domain, their separation by a stretch of hydrophobic amino acids suggest that they may lie on opposite sides of a membrane. The two *unc-84* deletion alleles, *e1174* and *n322*, but no others, have semi-dominant effects (data not shown). This finding is consistent with the hypothesis that *unc-84* dimerizes, in which case the *e1174* and *n322* mutant UNC-84 proteins could interfere with wild-type UNC-84 function. Dimerization could also account for the intragenic complementation of class 3 and class 4 *unc-84* alleles.

The C-terminal domain defined by the class 3 alleles is conserved in *C. elegans*, *S. pombe* and mammals. We call this domain SUN. Three of the four alleles that abolish UNC-84 C-terminal function affect two amino acids that are conserved among SUN proteins. In addition, all four genes with the SUN domain contain a predicted transmembrane domain. These data suggest that the biochemical function of the SUN domain is conserved and that the function of the domain may require proximity to a membrane. Based on the localizations of the

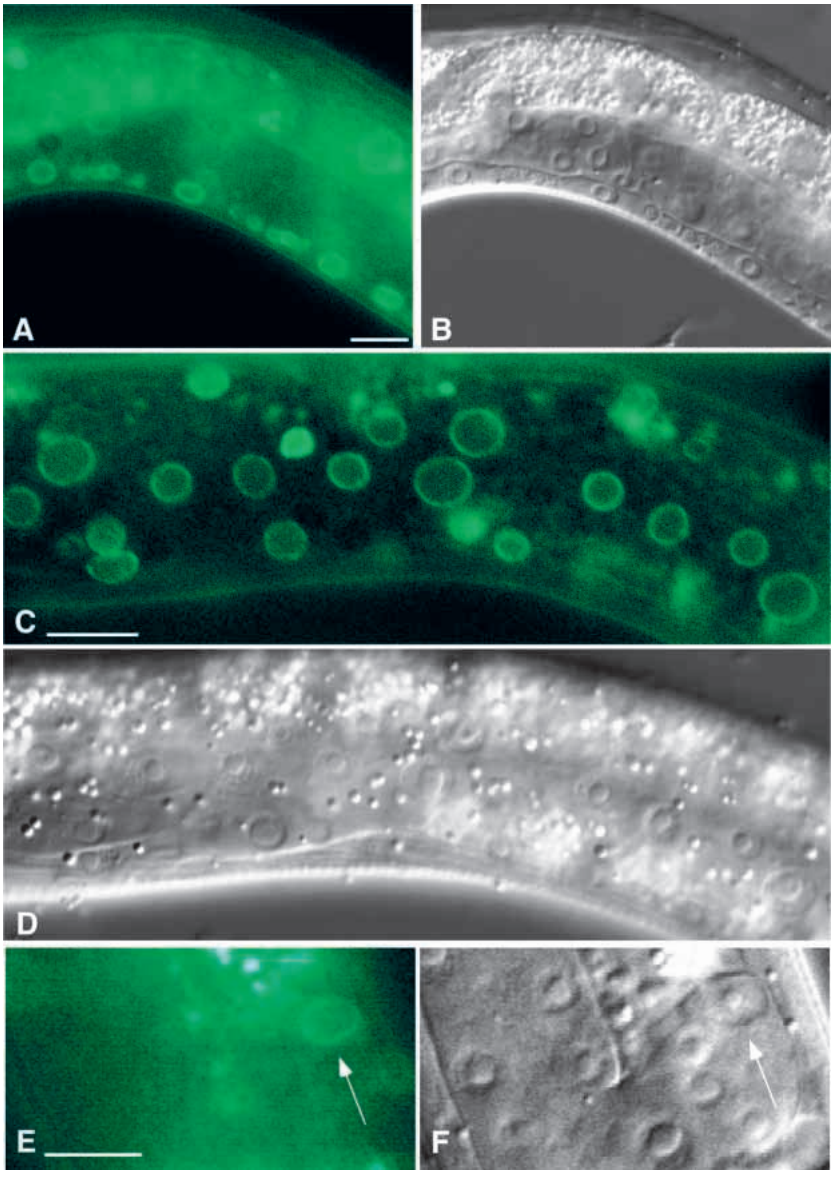

Fig. 6. Functional UNC-84A::GFP is ubiquitously expressed and localized to the nuclear periphery. (A) A fluorescence and (B) a Nomarski image, of neuronal, hypodermal, uterine and intestinal nuclei expressing UNC-84A::GFP. All somatic nuclei shown express the reporter construct. Bar, 10 μm. (C) A fluorescence and (D) a Nomarski image, of the lateral surface of an UNC-84A::GFP expressing larva showing ubiquitous expression in hypodermal cells. Bar, 10 μm. (E) A fluorescence and (F) a Nomarski image, of a migrating distal tip cell (white arrow). UNC-84A::GFP does not appear to be expressed in the germline, as is commonly observed for *C. elegans* transgenes (Kelly et al., 1997). Bar, 5 μm.

UNC-84::GFP fusion protein and the Sad1 protein (Hagan and Yanagida, 1995), we propose that this membrane is the nuclear envelope.

UNC-84 has functions associated with UNC-83 and ANC-1

The phenotypic analyses of *unc-84*, *unc-83* and *anc-1* mutant animals suggest a complex role for *unc-84* in nuclear migration, nuclear anchoring and gonad migration. Putative null mutations of *unc-84* cause temperature sensitive defects in both nuclear migration and gonadal migration indistinguishable from the defects caused by *unc-83* mutations. However, unlike most *unc-84* mutants, *unc-83* animals and *unc-84* class 4 animals are not abnormal in nuclear anchoring. By contrast, *anc-1* animals are abnormal in nuclear anchoring but do not display any gross nuclear or gonadal migration defects. These data suggest a model for *unc-84* function. The N- and C-termini of UNC-84A are both required for nuclear and gonadal migration, especially at higher temperatures, and they act in conjunction with UNC-83 but not with ANC-1. In addition, the C terminus of UNC-84A is required for nuclear anchoring in conjunction with ANC-1 but not with UNC-83.

All alleles of *unc-83* and *unc-84*, regardless of their affects on nuclear anchoring, cause defects in DTC migration, which suggests that the functions of *unc-83* and *unc-84* in nuclear migration but not in nuclear anchoring are important for DTC migration. Interestingly, the DTC migration is distinctive in that its nucleus is closely associated with the leading edge of the cell as opposed to the trailing edge (E. Hedgecock, personal communication). Defects in interpreting spatial or temporal cues typically affect a particular step of DTC migration (Hedgecock et al., 1987). The broader nature of the *unc-84* gonadal migration defect suggests that the migratory mechanism itself is abnormal.

UNC-84 may facilitate an interaction between the nucleus and centrosome

As proposed by Sulston and Horvitz (1981), P cells that fail to undergo nuclear migration may die because an essential component for cell viability is lost to the cytoplasmic extension in *unc-84* mutant P cells. Since the force for nuclear migration in the *Drosophila* syncytial blastoderm appears to be transmitted to the nucleus through the centrosome (Raff and Glover, 1989), perhaps the centrosome is the component required for the viability of the P cell during failed nuclear migration. UNC-84 may be an integral nuclear envelope protein involved in an interaction between the centrosome and the nucleus. Interestingly, *S. cerevisiae*, which maintains its spindle pole body embedded in the nuclear envelope during all stages of the mitotic and meiotic cell cycle (Byers, 1981), does not encode a SUN domain within its genome. This finding is consistent with the hypothesis that the SUN domain mediates the nuclear-centrosomal interaction.

We thank A. McGee for assistance with the cloning of *unc-84* and D. Starr for some of the seam cell marker double mutant strains. We thank E. Hedgecock and J. Thomas for *unc-84* alleles, P. Okkema and A. Fire for the cDNA library, A. Fire and A. Coulson for DNA clones and M. Sundaram for the RNA blot. We thank D. Fay, W. Hanna-Rose, D. Starr and J. Yochem for critical reading of the manuscript. C. M. was a National Defense Science and Engineering Graduate Fellow. M. H. was a Lucille P. Markey Scholar and a Searle Scholar. This work was supported by National Institutes of Health grants GM24663 (to H. R. H.) and GM47869 (to M. H.). H. R. H. is an Investigator and M. H. is an Assistant Investigator of the Howard Hughes Medical Institute.

REFERENCES

Altschul, S. F., Madden, T. L., Schaffer, A. A., Zhang, J., Zheng, Z., Miller, W. and Lipman, D. J. (1997). Gapped BLAST and PSI-BLAST: a new generation of protein database search programs. *Nucleic Acids Res.* **25,** 3389-3402.

Boguski, M. S., Lowe, T. M. and Tolstoshev, C. M. (1993). dbEST–database for 'expressed sequence tags'. *Nat. Genet.* **4,** 332-333.

Brenner, S. (1974). The genetics of *Caenorhabditis elegans*. *Genetics* **77,** 71-94.

Byers, B. (1981). Cytology of the yeast life cycle. *In The Molecular Biology of the Yeast* Saccharomyces*: Life Cycle and Inheritance* (ed. J. Stathern, E. W. Jones and J. R. Broach), pp. 59-96. Cold Spring Harbor Laboratory, Cold Spring Harbor, NY.

Ellis, H. M. and Horvitz, H. R. (1986). Genetic control of programmed cell death in the nematode *Caenorhabditis elegans*. *Cell* **44,** 817-829.

Fan, S. and Ready, D. F. (1997). *Glued* participates in distinct microtubule-based activities in *Drosophila* eye development. *Development* **124,** 1497-1507.

Fischer-Vize, J. A. and Mosley, K. L. (1994). *marbles* mutants: uncoupling cell determination and nuclear migration in the developing *Drosophila* eye. *Development* **120,** 2609-2618.

Gu, T., Orita, S. and Han, M. (1998). *C. elegans* SUR-5, a novel but conserved protein, negatively regulates LET-60 Ras activity during vulval induction. *Mol. Cell. Biol.* **18,** 4556-4564.

Hagan, I. and Yanagida, M. (1995). The product of the spindle formation gene *sad1+* associates with the fission yeast spindle pole body and is essential for viability. *J. Cell Biol.* **129,** 1033-1047.

Han, M. and Sternberg, P. W. (1990). *let-60*, a gene that specifies cell fates during C. elegans vulval induction, encodes a ras protein. *Cell* **63,** 921-931.

Hedgecock, E. M., Culotti, J. G. and Hall, D. H. (1990). The *unc-5, unc-6,* and *unc-40* genes guide circumferential migrations of pioneer axons and mesodermal cells on the epidermis in *C. elegans*. *Neuron* **2,** 61-85.

Hedgecock, E. M., Culotti, J. G., Hall, D. H. and Stern, B. D. (1987). Genetics of cell and axon migration in *Caenorhabditis elegans*. *Development* **100,** 365-382.

Hedgecock, E. M. and Thomson, J. N. (1982). A gene required for nuclear and mitochondrial attachment in the nematode *Caenorhabditis elegans*. *Cell* **30,** 321-330.

Hirsh, D., Oppenheim, D. and Klass, M. (1976). Development of the reproductive system of *Caenorhabditis elegans*. *Dev. Biol.* **49,** 200-219.

Horvitz, H. R. and Sulston, J. E. (1980). Isolation and genetic characterization of cell-lineage mutants of the nematode *Caenorhabditis elegans*. *Genetics* **96,** 435-454.

Kelly, W. G., Xu, S., Montgomery, M. K. and Fire, A. (1997). Distinct requirements for somatic and germline expression of a generally expressed *C. elegans* gene. *Genetics* **146,** 227-238.

Kimble, J. and Hirsh, D. (1979). Post-embryonic cell lineages of the hermaphrodite and male gonads in *Caenorhabditis elegans*. *Dev. Biol.* **70,** 396-417.

Kozak, M. (1984). Compilation and analysis of sequences upstream from the translational start site in eukaryotic mRNAs. *Nucl. Acids Res.* **12,** 857-872.

Krause, M. and Hirsh, D. (1987). A trans-spliced leader sequence on actin mRNA in *Caenorhabditis elegans*. *Cell* **49,** 753-761.

Mello, C. and Fire, A. (1995). DNA Transformation. *In* 'C. elegans: *Modern Biological Analysis of an Organism*' (ed. H. F. Epstein and D. C. Shakes), pp. 452-480. Academic Press, San Diego.

Morris, N. R., Ziang, X. and Beckwith, S. M. (1995). Nuclear migration advances in fungi. *Trends in Cell Biol.* **5,** 278-282.

Oakley, B. R. and Morris, N. R. (1980). Nuclear movement is β-tubulin dependent in *Aspergillus nidulans. Cell* **19,** 255-262.

Okkema, P. and Fire, A. (1994). The *Caenorhabditis elegans* NK-2 class homeoprotein CEH-22 is involved in combinatorial activation of gene expression in pharyngeal muscle. *Development* **120,** 2175-2186.

Orita, S., Sasaki, T., Naito, A., Komuro, R., Ohtsuka, T., Maeda, M., Suzuki, H., Igarashi, H. and Takai, Y. (1995). Doc2: a novel brain protein having two repeated C2-like domains. *Biochem. Biophys. Res. Commun.* **206,** 439-448.

Raff, J. W. and Glover, D. M. (1989). Centrosomes, and not nuclei, initiate pole cell formation in Drosophila embryos. *Cell* **57,** 611-619.

Reinsch, S. and Gonczy, P. (1998). Mechanisms of nuclear positioning. *J. Cell Sci.* **111,** 2283-2295.

Steinberg, G. (1998). Organelle transport and molecular motors in fungi. *Fungal Genet. Biol.* **24,** 161-177.

Sullivan, D. S. and Huffaker, T. C. (1992). Astral microtubules are not required for anaphase B in *Saccharomyces cerevisiae*. *J. Cell Biol.* **119,** 379-388.

Sulston, J. and Horvitz, H. R. (1977). Post-embryonic cell lineages of the nematode, *Caenorhabditis elegans*. *Dev. Biol.* **56,** 110-156.

Sulston, J. E. (1976). Post-embryonic development in the ventral cord of *Caenorhabditis elegans*. *Philos. Trans. R. Soc. Lond. B Biol. Sci.* **275,** 287-298.

Sulston, J. E. and Horvitz, H. R. (1981). Abnormal cell lineages in mutants of the nematode *Caenorhabditis elegans*. *Dev. Biol.* **82,** 41-55.

Sulston, J. E., Schierenberg, E., White, J. G. and Thomson, J. N. (1983). The embryonic cell lineage of the nematode *Caenorhabditis elegans*. *Dev. Biol.* **100,** 64-119.

Terns, R. M., Kroll-Conner, P., Zhu, J., Chung, S. and Rothman, J. H. (1997). A deficiency screen for zygotic loci required for establisment and patterning of the epidermis in *Caenorhabditis elegans*. *Genetics* **146,** 185-206.

Thompson, J. D., Higgins, D. G. and Gibson, T. J. (1994). CLUSTAL W: improving the sensitivity of progressive multiple sequence alignment through sequence weighting, position-specific gap penalties and weight matrix choice. *Nucleic Acids Res.* **22,** 4673-4680.

Trent, C., Tsung, N. and Horvitz, H. R. (1983). Egg-laying defective mutants of the nematode *Caenorhabditis elegans*. *Genetics* **104,** 619-647.

Waterston, R. and Sulston, J. (1995). The genome of *Caenorhabditis elegans*. *Proc. Natl. Acad. Sci. USA* **92,** 10836-10840.

Welte, M. A., Gross, S. P., Postner, M., Block, S. M. and Wieschaus, E. F. (1998). Developmental regulation of vesicle transport in Drosophila embryos: forces and kinetics. *Cell* **92,** 547-557.

Williams-Masson, E. M., Heid, P. J., Lavin, C. A. and Hardin, J. (1998). The cellular mechanism of epithelial rearrangement during morphogenesis of the *Caenorhabditis elegans* dorsal hypodermis. *Dev. Biol.* **204,** 263-276.